Simple coincidence detection in tonic and phasic LIF neurons

Zach Danial

Intro to Neuronal Modeling, Fall 2020

Abstract

Coincidence detection by neurons is a process that allows individual neurons to compute time differences in the arrival of signals. Auditory brain stem neurons found in the medial superior olive are particularly good at coincidence detection, which contributes to the emergent capability of sound localization. [Izhikevich, 2000] describes detecting these time differences as action potentials generated from the accumulation of voltage from distinct pairs of signals arriving sequentially. While this intuitively explains how coincidence detection functions, it does not give us much insight into its qualitative properties.

[Meng et al., 2012] goes very in-depth into the features of coincidence detection in the Rothman and Mannis model for half-wave rectified sinusoidal inputs distinguished by a difference in phase. In this project, we formulate coincidence detection in perhaps its simplest possible form (leaky-integrate-and-fire neurons with dirac-delta current injections), allowing us to solve for the firing condition analytically. We then switch to a phasic neuron (by including low-voltage adaptation) to explore a slightly more complex case.

There are two goals in building coincidence detection up from its simplest form: the first is to make the concept and its implications more accessible, the second is to have a simplified analytical framework with the potential to generate results that still hold in more complex models.

1 Introduction

Sound localization, the ability of many animals to determine the location of a source of sound (even without being able to see it), is a fascinating inborn ability. Research has pointed to neurons in the auditory brain stem that individually can compute the time differences between the arrival of the sound wave at each ear. These inter-aural time difference carry the information of the angle of the source to the animal or person.

This computation is referred to in the literature as **coincidence detection** (CD) – simply put, detecting the time differences (TDs) in the arrival of two stimuli. Neurons in the medial superior olive (MSO) are known to perform this

computation specifically for the purpose of sound localization. While CD has a long history in the neuroscience literature, much of the work focuses on computational and numerical simulations within high-dimensional neuronal models. The drawback is two-fold: (1) this constricts the accessibility of understanding CD and the results, which differ based on the number and accuracy of dimensions; (2) we lose the use of symbolic manipulation, which constrains the space of possible phenomena to search for, making results easier to extract.

[Meng et al., 2012] analyzes CD in a number of models for half-wave rectified sinusoidal inputs distinguished by a difference in phase. In this paper we start by formulating CD in arguably its simplest possible form: Dirac-delta functions as current inputs into a leaky integrate and fire neuron. As we progress, we add levels of realism to the model, and compare the changes as we move forward.

2 Methods and Results

2.1 Leaky Integrate and Fire (tonic)

We begin by formulating the condition for CD within the dimensionless LIF model using Dirac-delta pulses to represent incoming signals. With $v = V_{th} - V_{rest}$, we consider the following differential equation for the LIF neuron's voltage:

$$\dot{v} = -v + i(t), v \in [0, \theta = 1], \tag{1}$$

with the condition that $v(t^+_{fire}) = 0$, where t_{fire} is such that $v(t_{fire}) = \theta = 1$. We construct our input current as the sum of two signals, of charge q and $k \cdot q$, arriving at t_1 and t_2, respectively:

$$i(t) = q[\delta(t - t_1) + k \cdot \delta(t - t_2)]; \quad q \in (0, 1), k \in (0, \frac{1}{q}) \tag{2}$$

The intervals for q, k arise from the requirement that neither input should cause the neuron to fire individually. Integrating 1 tells us that $v(t_1) = q$ and $v(t_2) = q \exp(t_1 - t_2) + kq$. We define $\tilde{t} := t_2 - t_1$ as the TD between stimulus arrival, and pose the *firing condition* in terms of $\tilde{t}$. The *firing condition* $v(t_2) \geq \theta => q \exp(-\tilde{t}) + kq \geq 1$ allows the LIF neuron to distinguish between stimulus arrival differences greater than or less than $\tilde{t}$, if

$$\tilde{t} \leq \ln(\frac{q}{1 - kq}). \tag{3}$$

This threshold is computed for $q, kq \in (0, 1)$ in the right panel of Figure 1. There is a threshold $kq = 1 - q$, below which there are no action potentials. Note the asymmetry in $\tilde{t}$ with respect to the magnitude of the two stimuli. This feature is expected as the two stimuli are separated by time within a time dependent system.

The left panel of Figure 1 considers the case of two incoming signals with the same magnitude ($k = 1$). In this simplest result we observe detection of

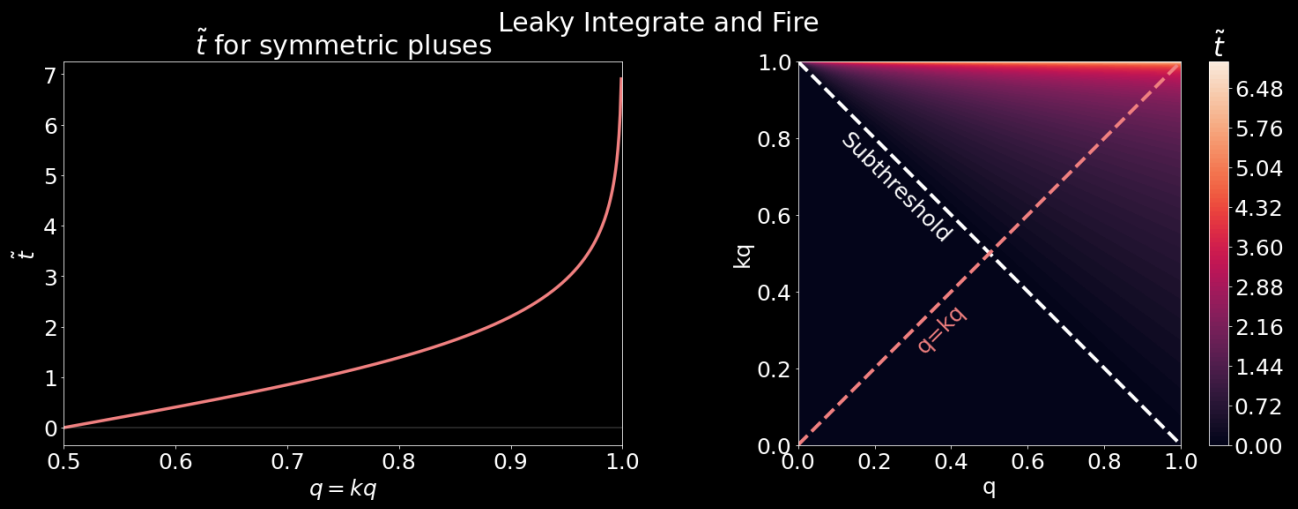


Figure 1: *The left panel shows how the threshold TD ($\tilde{t}$) changes based on two incoming stimuli of the same amplitude. The neuron will only fire if the TD between the arrival of the two stimuli is less than $\tilde{t}$. The right panel shows the same information within a heatmap, but for any pair of two magnitudes $\in [0, 1]$. The symmetric case is highlighted (dashed pink line). Note that any pairs (q, kq) below the white dashed line cannot cause the neuron to fire no matter how close in time.*

time intervals $\in [0, \infty]$. As we will see, this breaks down in even a marginally more realistic model; however, the logarithmic increase of $\tilde{t}$ with respect to a function of the inputs remains.

In the next section we take a small step towards realism, and reformulate the problem including threshold adaption.

2.2 LIF with Sub-threshold Adaptation

We now consider the inclusion of threshold adaption and its effects on the problem of coincidence detection. We model the phasic neuron governed by the following system of differential equations:

$$\dot{v} = -v + i(t) \tag{4}$$

$$\dot{\theta} = \frac{(\alpha v + 1 - \theta)}{\tau_\theta}, \quad \alpha > 0 \tag{5}$$

Again, $i(t)$ described by equation 2 means that $v(t_1^+, t_2^-) = q \exp(t_1 - t)$. However, a dynamic θ means that we need to account for the changes in the threshold induced by v. By integrating $\int_{t_1}^{t_2^-} \frac{d\theta}{dt}(t_1^+, t_2^-) = \frac{1}{\tau_\theta}(\alpha q \exp(t_1 - t) + 1 - \theta)$ with the initial condition $\theta(t_1^-) = 1$, we resolve that $\theta(t_2^-) = \frac{\alpha q}{\tau_\theta - 1}[exp(\frac{\tilde{t}}{\tau_\theta}) - exp(\tilde{t})] + 1$.

This leads us directly to our new *firing condition*:

$$q\exp(-\tilde{t}) + kq \geq \frac{\alpha q}{\tau_\theta - 1}[exp(\frac{\tilde{t}}{\tau_\theta}) - exp(\tilde{t})] + 1 \tag{6}$$

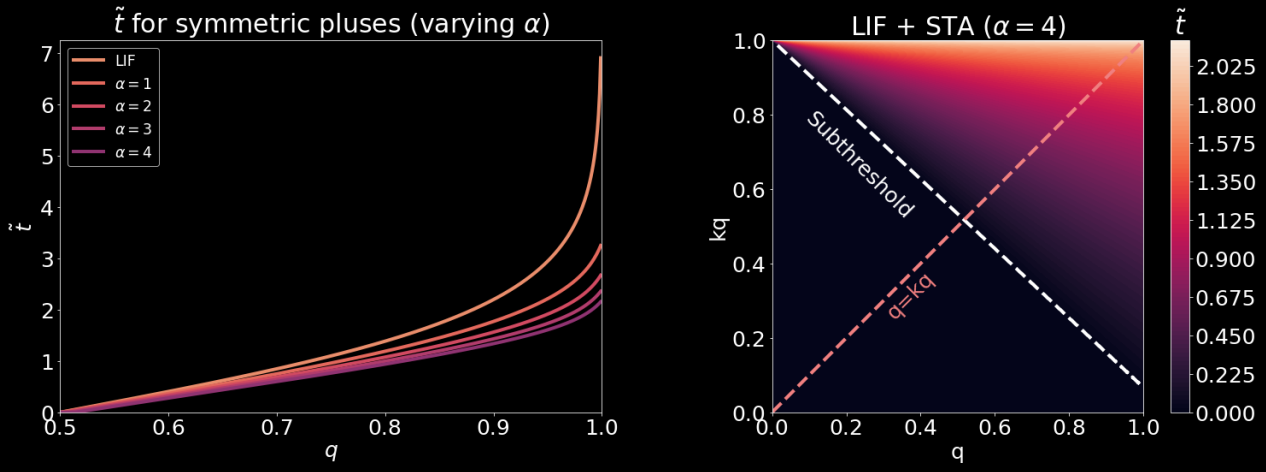


Figure 2: *The left panel shows how the threshold TD ($\tilde{t}$) changes as we vary the magnitude of adaptation (Note: LIF+STA reduces to LIF when $\alpha = 0$). The neuron will only fire if the TD between the arrival of the two stimuli is less than $\tilde{t}$. The interval of measurable TDs is no longer infinite, but is now determined by the degree of adaptation. The right panel is a heatmap for any pair of two magnitudes $\in [0, 1]$. The symmetric case is highlighted (dashed pink line). Note that any pairs (q, kq) below the subthreshold line (white dashed) cannot cause the neuron to fire no matter how close in time. The slope of the subthreshold line has increase with the addition of adaptation, meaning that some (q, kq) pairs no longer cause action potentials.*

In order to solve equation 6 we resort to Newton's method for $f(\tilde{t}) = q\frac{\alpha}{\tau_\theta - 1}[\exp(\frac{-\tilde{t}}{\tau_\theta}) - \exp(-\tilde{t})] - q\exp(-\tilde{t}) + (1 - kq) = 0$. We consider the case $\tau_\theta \gg \tilde{t}$, which allows us to use $q\frac{\alpha}{\tau_\theta - 1}[1 - \exp(-\tilde{t})] - q\exp(-\tilde{t}) + (1 - kq) = 0$ in order to form our initial guess t_0 as:

$$\tilde{t}_0 = -ln(\frac{1 - kq}{q(1 + \frac{\alpha}{\tau_\theta - 1})} + 1 - \frac{1}{1 + \frac{\alpha}{\tau_\theta - 1}}) \tag{7}$$

$$\tilde{t}_{n+1} = \tilde{t}_n - \frac{f(\tilde{t})}{f'(\tilde{t}_n)} \tag{8}$$

Note (for ease, speed, and accuracy of computation) that $f'(\tilde{t}) = 1 - kq - f(\tilde{t})$. Using equations 7 and 8 we produce Figure 2, which allows us to compare the results of the modelling approaches of Sections 2.1 and 2.2. The right panel of Figure 2 is markedly different than that of Figure 1. As reflected in the left panel, $\tilde{t}$ rises much slower and now features a finite range of distinguishable values, an interval which is dependent on adaptation. Again, we observe the logarithmic

increase of $\tilde{t}$ with respect to a function of the inputs. Additionally, the slope of the line marking sub-threshold stimulus pairs has marginally increased, moving some pairs (q, kq) to the sub-threshold regime.

Next we will add another level of realism to the model, changing our methodology and analysis to suit the nuances of this new case.

2.3 Considering alternative inputs

We now consider a different construction of $i(t)$ to make the point that even these simple formulations can exhibit a similar range of behaviors to more complicated models. We implement a modified form of the α-function $[f(t) = \alpha t \exp(1-\alpha t)]$ in order to construct two signals (s_1, s_2) with symmetric amplitude (A) shifted by a TD Δp.

$$\mathrm{s}_1(t) = At \cdot \exp(1-t)$$
$$\mathrm{s}_2(t) = A(t-\Delta p) \cdot \exp(1-(t-\Delta p))$$

$$i(t) = s_1(t) + s_2(t) \tag{9}$$

We again require the constraint that neither signal is capable of individually causing the neuron to fire. Through simulating for a range of amplitude values A (up to 2 decimal points), $A = 1.54$ was identified as a close lower bound for the maximum.

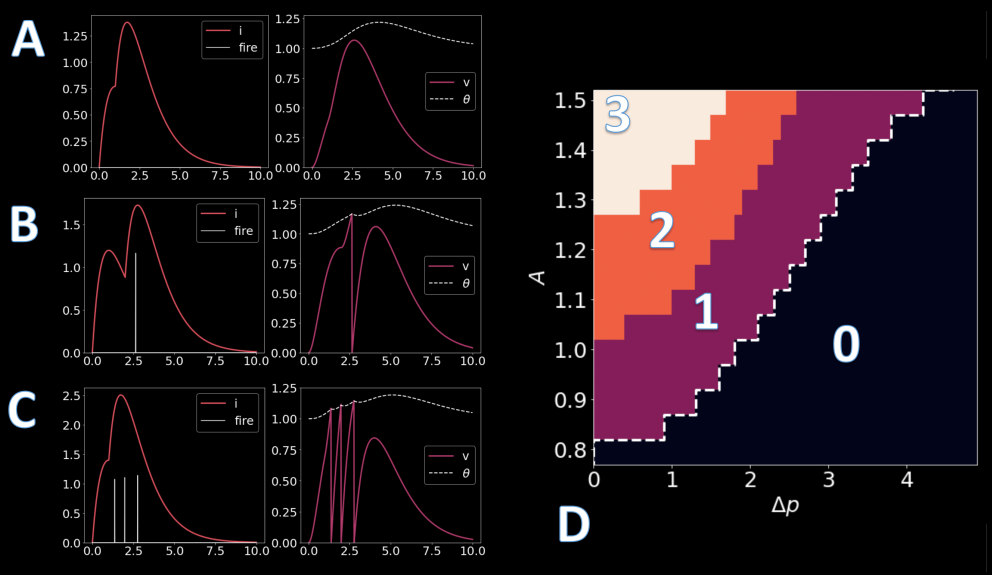


Figure 3: *Plots A, B, and C are samples of the behavior around the parameter space. All feature time on the x-axis and voltage on the y-axis. The left panel show the input current i, and the action potentials (fire). The right panel shows the time-course of the voltage v and threshold θ. We show the following samples: A) near threshold but no firing; B) one actional potential; C) bursting. Plot D explores the parameter space of TD (Δp) and amplitude (A), with regions highlighted based on the number of action potentials in response to the two signals.*

All the results of this section are from numerical simulations using equations 4, 5 and 9.

As shown in [Meng et al., 2012], there are areas of the parameter space that result in a burst of action potentials per cycle of the half-rectified sinusoidal inputs within a number of phasic neuron models. Figure 3 showcases a similar behavior in the case of LIF+STA with $i(t)$ as described in equation 9. Even with the constraint that neither signal individually causes an action potential, we find regions of the parameter space that correspond to firing bursts of up to three spikes.

We introduce Δp in this section to account for the ambiguity in the *arrival time* of the stimuli. As opposed to sections 2.1 and 2.2, the arrival of each stimulus is not defined by a distinct point of arrival, but rather by the onset of the stimulus (closest to the event) and the peak of the stimulus (easiest to detect by the soma). From here on we consider the stimulus arrival times to be defined by the peak of the respective stimulus, which occur at $t = 1$ and $t = 1 + \Delta p$, respectively. This is important because if the first stimulus brings voltage close enough to the threshold, the neuron will fire at the onset of the second signal – which begs the question of how a neuron can identify that there are really two discrete signals. Thus we inquire about $\tilde{t}$ redefined as the time of first firing, and its error to the ground truth arrival of the second stimulus $(1 + \Delta p)$.

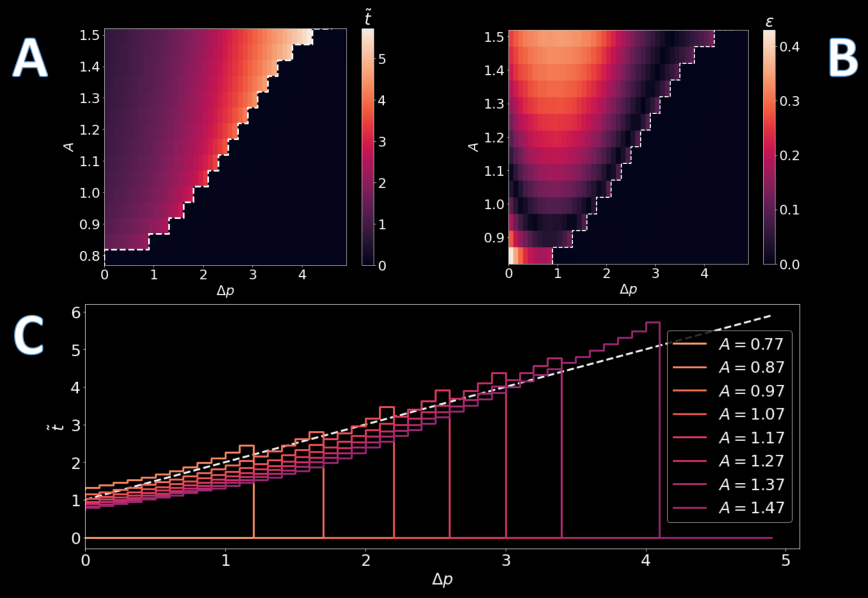


Figure 4: *Plot A explores the parameter space showing the time of first firing ($\tilde{t}$) for TD (Δp) and amplitude (A). Considering this as a measure of the arrival of the second stimulus, plot B shows the percentage error of ($\tilde{t}$) from ground truth ($1+\Delta p$). While the region of high error seems large, plot B/C shows that we can tune accuracy by changing amplitude.*

Figure 4 shows the results of this analysis. In plot (B) we see that for most of the parameter space, the percentage error is high, but there is a continuous region of very high accuracy. This suggests that neurons would need to be tuned for detecting a very narrow interval of TDs. Additionally, it should be noted that the low amplitude region features two areas of high-accuracy, which would be very interesting if still featured in more biophysically accurate models. While the percentage errors seem very high, in plot (C) we observe that the results are qualitatively accurate when considering the inherent non-linearity inherent in $\tilde{t}$, which is now trying to approximate a linear function.

3 Discussion

The result of this study is a toy model of CD that introduces the phenomena in a mathematical framework that allows for some basic analysis while still reproducing some of the phenomena present in purely computational models. From this framework, we learn something significant about CD that may or may not hold up in more biophysically accurate models: the TDs a neuron can measure are determined by the magnitude of the input stimuli. This points to the idea that dendritic attenuation may be the controller of the time-differences to which a given neuron is tuned. This would link the structure of the MSO cell's dendrites to its function within the sound localization paradigm.

Although the model reproduces some of the more advanced phenomena, an interesting extension of this work would be to check its validity with respect to biophysically accurate models. If so, further analytical advances could be made, and rechecked for validity. While sections 2.2 and 2.3 involve computation, in both cases we can get halfway to the final results analytically, which allows searching for results in different directions than considered in this paper.

References

[Izhikevich, 2000] Izhikevich, E. M. (2000). Neural excitability, spiking and bursting. *International journal of bifurcation and chaos*, 10(06):1171–1266.

[Meng et al., 2012] Meng, X., Huguet, G., and Rinzel, J. (2012). Type iii excitability, slope sensitivity and coincidence detection. *Discrete and continuous dynamical systems. Series A*, 32(8):2729.

[Rinzel and Huguet, 2013] Rinzel, J. and Huguet, G. (2013). Nonlinear dynamics of neuronal excitability, oscillations, and coincidence detection. *Communications on pure and applied mathematics*, 66(9):1464–1494.